Two-step synthesis of polymer fibre material comprising indium-, bismuth-, or antimony-doped nanosized tin oxides

I Lysak[1], G Lysak and T Malinovskaya

Siberian Physical Technical Institute, *Tomsk State University*, 1 Novosobornaya Square, Tomsk 634050, Russian Federation

[1]E-mail: lysakilya@gmail.com

Abstract. In this paper, we present a method of formation of polymer fibre materials comprising dispersed oxides of rare and trace elements. The results of X-ray diffraction and spectral analyses show that the optimum synthesis conditions of the antimony-doped tin oxide, indium-doped tin oxide, and bismuth-doped tin oxide particles are provided using the "reverse" hydrolytic co-precipitation of hydroxides from chloride solutions combined with the subsequent thermal treatment at 1000°C. Durable fixation of nanoparticles on the fibre surface is confirmed by the atomic emission spectrometry with inductively coupled plasma and transmission electron microscopy. The results show that spraying of a free stream of the thermoplastic polymer melt with a gas stream containing nanoparticles allows obtaining fibre materials, which possess catalytic, photosensitive, as well as heat and sound insulating properties.

1. Introduction

Nowadays, materials comprising disperse oxides of rare and trace elements (RTE) are widely used in a variety of fields of science and technology to create catalytic, photosensitive, heat and sound insulating elements [1]. The use of "metal-insulator-semiconductor" structures as selective coatings to maintain certain thermal regime of objects in modern optical communication systems for the recording of infrared radiation, as well as in devices for photocatalytic degradation of organic pollutants is caused by low values of fixed charge in dielectrics (Q_g), high surface density of electronic states at the semiconductor – insulator boundary (N_{ss}), long relaxation times of excess concentration of minority charge carriers (τ_s), and high values of the dielectric strength [2]. Functional characteristics of oxide materials based on RTE depend largely on the synthesis mechanisms and structural phase transitions occurring in the material at various stages of its fabrication. The synthesis process of such materials is an extremely complex task that requires strict compliance with the ratio of initial components, the sequence of operations and the parameters of technological processes. One of the main methods of obtaining products for solid-phase synthesis of disperse oxides of RTE is the hydrolytic method [3]. This method allows to widely vary properties of the resulting materials and to achieve a significant interaction and dispersion at a specified ratio of components. Generally, the considered class of compounds is used in the form of thin films of RTE oxides such as In_2O_3, SnO_2, CdO, ThO_2, MoO_3, ZnO, WO_3, Bi_2O_3, ZrO_2, and V_2O, often doped with Sn, Sb, Bi, Mo, B, Te, W, Ti, Fe, F, or Zn [4-5]. However, for creating heat insulating materials and filters, the reinforcing bases for the composite hulls of yachts, aircrafts, and cars, as well as the catalytic and bactericide systems, attachment of these particles on the surface of the polymer fibre materials is promising [6-10].

Thus, the goal of this work was to study chemical and structural phase transitions occurring at different stages of synthesis of the oxide Sn-Sb-O, Bi-Sn-O, and In-Sn-O systems depending on the conditions and methods of its implementation, and then, to develop a two-step process for producing a polymer fibre material comprising disperse oxides of rare and trace elements on the surface using the spraying method.

2. Experimental

As raw materials, the polypropylene PP H080 GP grade issued in accordance with the engineering specifications TU 2211-103-70353562-2013 ed. 3 (Russia) and the antimony-doped tin oxide, indium-doped tin oxide, and bismuth-doped tin oxide nanoparticles (ATO, ITO, and BTO, respectively) were used. ATO, ITO, and BTO materials were produced using a solid-phase synthesis method in the temperature range 300-1473 K. The reaction mixtures were obtained using the hydrolytic method based on the co-precipitation of Sn (II, IV), Sb (III), Bi (III), or In (III) from the nitrate and chloride solutions with an alkaline reagent. Co-precipitation of Sn (II, IV), Sb (III), or In (III) was performed either by the "direct" (reaction of neutralisation of an acidic solution with an alkaline reagent) or "reverse" (reaction of neutralisation of an alkaline reagent with acidic solutions) methods. Chemical composition of raw materials and products of the hydrolytic deposition are presented in table 1 for the tin oxides synthesis.

Table 1. Chemical composition of raw materials and products of hydrolytic deposition.

System	Raw materials	Products of hydrolytic deposition	Fabrication method
Sn - Sb - O	$SnCl_4 \cdot 5H_2O$ + 1M HCl Sb_2O_3 + 9M HCl NH_4(Na)OH (3-6M)	Product I $[\{SnO_2\}Sn(OH)_4] + Sb^{+3}/Cl$	"Direct" hydrolytic
	- // -	Product II $[\{SnO_2\}Sn(OH)_4] + Sb^{+3}$	"Reverse" - // -
	Sn + SnO_2 + 9M HCl Sb_2O_3 + 9 M HCl NH_4(Na)OH (3-6 M)	Product III $Sn_3O_2(OH)_2 + Sb^{+3}/ Cl^-$	"Direct" - // -
	- // -	Product IV $Sn_3O_2(OH)_2 + Sb^{+3}$	"Reverse" - // -
Sn -Bi - O	Sn + Bi_2O_3 + 9M HNO_3 NH_4(Na)OH (3-6M)	Product I $Bi_2Sn_2O_5(OH)_4 \cdot 2H_2O$	"Direct" hydrolytic
	$SnCl_4 \cdot 5H_2O$ + 1M HCl Bi_2O_3 + 9M HCl NH_4(Na)OH (3-6M)	Product II $[\{SnO_2\}Sn(OH)_4]$ + BiOCl	- // -
In-Sn-O	In_2O_3 + 9M HNO_3 Sn + 1M HNO_3 NH_4OH (3-6M)	Product I $In(OH)_3/NO^- + Sn_3O_2(OH)_2 \cdot$	"Direct" hydrolytic
	$SnCl_4 \cdot 5H_2O$ + 1M HCl In_2O_3 + 9M HCl NH_4OH (3-6M)	Product II $[\{SnO_2\}Sn(OH)_4]$ + $In(OH)_3/Cl^-$	- // -

Polypropylene pellets were heated up to the temperature 265°C, which corresponds to the melt homogenisation. Afterwards, the melt was fed to the inlet nozzle of a spray-head [11, 12]. At the same time, the gas stream at a temperature about 20°C was fed under pressure to the spraying area through the convergent concentric nozzle. As a consequence, in the annular space between the polymer stream and the inlet nozzle wall, vacuum was produced and the ejected gas flow containing ATO, ITO or BTO nanoparticles appeared at a temperature of gas and particles about 20°C. Further, in the spraying

area, disintegration of the melt and the formation of the fibrous material occurred in the presence of oxide nanoparticles, which were deposited on the surface of the melt. Then, the fibrous material was solidified in a flow of ambient gas. The ATO nanoparticles and ITO or BTO nanoparticles were attached to its surface evenly and firmly.

To ensure a sufficient level of the research results reliability, mutually complementary physical, physicochemical, and chemical methods of material analysis were used. To identify the products of the solid-phase synthesis, X-ray diffraction analysis on a diffractometer Shimadzu XRD-6000 (CuK_α-radiation, reflection-based imaging geometry) with a scanning step of 0.02° within the 2Θ range of 10–80° at room temperature was used. An analysis of the phase composition, the sizes of the coherent scattering regions, and internal elastic stresses (Δd/d) was carried out using the full-profile analysis by a Powder Cell 2.5 computation program. The experimental diffraction patterns were smoothed over five points with a fast discrete Fourier transform algorithm (5pFFTFilter) [13-16]. The crystallite size and lattice microdistortions were determined from the broadening of the Bragg profile peaks. Analytical control of the deposition process and fixation of metal nanoparticles on the carrier, was implemented by atomic emission spectrometry with an inductively coupled plasma spectrometer ICAP 6300 Duo Thermo. The morphology and parameters of the size distribution of objects were studied by transmission electron microscopy (TEM) with a JEM-100CXII electron microscope. The sizes of objects were determined by the particle size distribution test followed by statistical processing of the results. The test samples for the transmission electron microscopy were prepared as follows: the fibre material comprising nanoparticles was milled and filled with distilled water. From the resulting mixture, a suspension was prepared. A drop of the suspension was placed on a preparative mesh with a pre-applied formvar film. The concentration of free charge carriers (*Ne*) in the material was determined from the plasmon resonance wavelength (λp).

3. Results and discussion

The basis of the hydrolytic preparation method of tin-antimony oxide materials is co-precipitation of tin(II, IV) and antimony(III). The effect of the reagent addition order on the physicochemical properties of synthesized materials (phase composition, structure, dispersion, the presence of impurities) was established. When using the "direct" hydrolytic synthesis, heat treatment of the co-precipitation products leads to the removal of the partial hydrolysis products built-in into the structure of initial gel from the matrix solution. In the “reverse” hydrolytic deposition, products free of impurities are formed. For instance, the method of the reverse order of the Sn(II) and Sb(III) co-precipitation from chloride solutions excludes the formation of toxic antimony compounds. Due to these peculiarities of the synthesis, in the heat-treated (above 600ºC) products of the "direct" co-precipitation, crystallites are formed that are smaller than those in the "reverse" co-precipitation products (figure 1). In addition, the sizes of crystallites of indium-doped tin oxide materials obtained from the chloride and nitrate solutions differ from each other. Regardless of the nature of reagents during solid-phase reactions in the antimony-doped tin oxide system with antimony concentration of 5-20 atomic %, the material crystallises in a tetragonal system with a defective rutile structure forming solid solutions. In the bismuth-doped tin oxide system with a bismuth concentration of 5-85 atomic %, no solid solutions are formed. If the atomic ratio of Bi:Sn = 1, only bismuth stannate of $Bi_2Sn_2O_7$ composition with a pyrochlore structure is produced. On changing the metal ratio of Bi:Sn, a biphasic mixture of the bismuth stannate and the corresponding oxide are formed. The monophasic bismuth stannate $Bi_2Sn_2O_7$ is formed by the hydrolytic method of Sn(IV) and Bi(III) co-precipitation from the nitrate solutions (figure 2). In the solid-phase synthesis of indium-doped tin oxide materials, a cubic modification of In_2O_3 structure with increased values of lattice spacings compared to the standard ones, or a two-phase mixture of this phase and a tetragonal modification of SnO_2 are formed. If tin content is increased up to 2 atomic % in the chloride solutions with pH6-9 and up to 12 atomic % in the nitrate solutions, high-temperature annealing at a temperature about 1000ºC results in the appearance of a SnO_2 phase in indium-doped tin oxide materials. An average crystallite size of In_2O_3

is an order of magnitude more than that for SnO_2. The use of initial components containing nitrate ions leads to the appearance of a hexagonal In_2O_3 phase and an $In_4Sn_2O_{12}$ phase (figure 3).

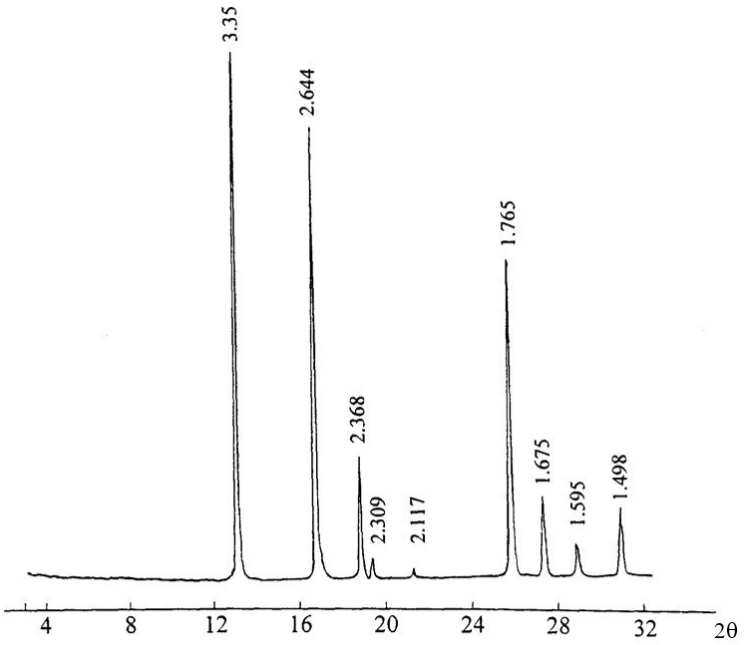

Figure 1. X-Ray diffraction of antimony (III) and tin (II, IV) co-precipitation products heat-treated at a temperature 1000°C: method – "all", antimony content – 20 atomic %

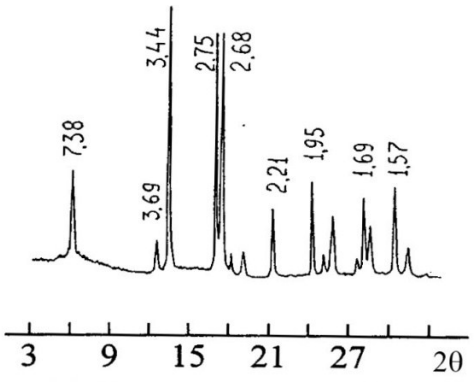

Figure 2. X-Ray diffraction of Bismuth (III) and tin(IV) co-precipitation products: method – "Direct" hydrolytic from the chloride solutions, the atomic ratio of Bi:Sn = 1, pH = 7

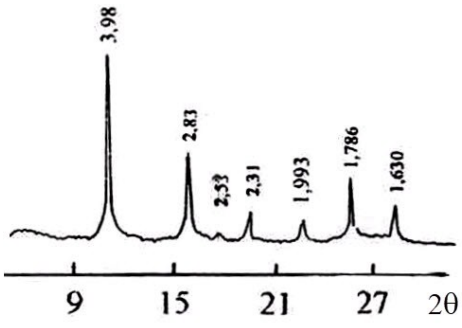

Figure 3. X-Ray diffraction of indium (III) and tin(IV) co-precipitation products: method – "Reverse", T_{cp} = 25°C, pH = 10, tin content – 1 atomic %

On the basis of the data on free charge carrier concentration (N_e) in the material, general regularities of degeneration of semiconductors caused by the physicochemical peculiarities of formation of semiconductor phases in the systems are identified. It is found out that deep degeneration of the semiconductor can be achieved only in the systems, which are characterised by the formation of substitutional solid solutions; the degeneracy depth is determined by the limit of mutual solubility of the components. For the Bi-Sn-O system, in which no formation of substitutional solid solutions is established, degeneration of the semiconductor is associated with the vacancy-type conductivity caused by the defectiveness of its crystalline structure. Solid solutions of antimony tin dioxide have

the maximum values of concentration of free charge carriers ~ $5.7 \cdot 10^{20}$ cm^{-3}. With increasing annealing temperature, an increase in the free electrons concentration is observed. When using Sn(II) and Sb(III) as the initial reagents obtained both by the mechanical mixing method and hydrolytic method, the maximum concentration N_e is achieved in the temperature range 550-670 K, wherein oxidation of Sn^{+2} is accompanied by the significant heat effect. In case of initial reagents Sn(IV) and Sb(III) at temperatures 470-770 K, N_e is low (~ 10^{17}-10^{18} cm^{-3}), which is associated with the sustained process of the SnO_2 crystallisation. At temperatures > 870 K, the formation of defect structure of tin dioxide is accompanied by an increase in the values of N_e. However, the maximum concentration ~ $5.7 \cdot 10^{20}$ cm^{-3} and the stability of this value are achieved only at temperatures of 1200-1470 K.

Based on these findings, optimal conditions for the synthesis of ATO and ITO materials are determined in the aspect of environmental safety and thermodynamic stability of materials as well as for the achievement of a predetermined concentration of free charge carriers in these materials. In particular, we recommend using the "reverse" hydrolytic co-precipitation of hydroxides of chloride solutions followed by the heat treatment of the gel at temperatures up to 1000°C. In this case, high degree of environmental safety is provided by the low content of the partial hydrolysis products in the original gel obtained by the "reverse" hydrolytic process. The control of the process conditions allows obtaining a material with an average crystallite size of 20 to 100 nm. These nanoparticles were used in fabrication of fibrous material. Based on the results of transmission electron microscopy (figure 4), it can be argued that disperse oxides are localised on the fibre surface in the form of clusters of arbitrary shape and cover from 10 to 25% of the surface area.

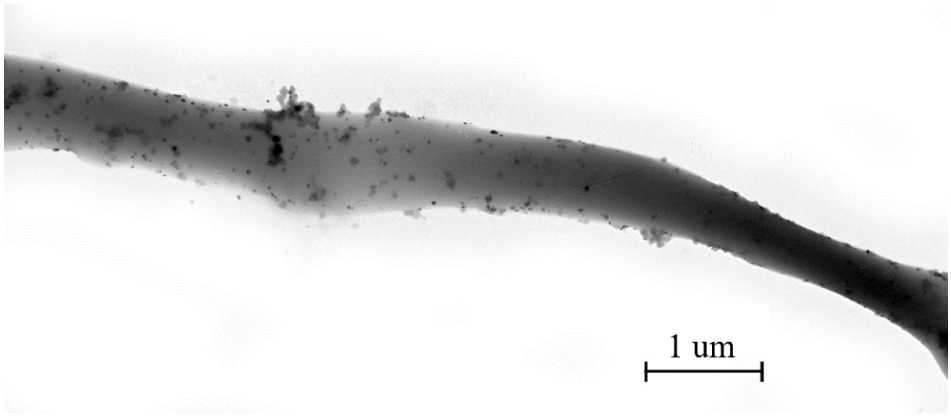

Figure 4. Fragment of a polypropylene fibre with oxide nanoparticles attached to its surface.

During the experimental verification of the proposed approaches fibres were formed from polypropylene in the presence of ATO nanoparticles. The air was supplied to a convergent annular nozzle of the fiber-forming ejection device under pressure P_{air} = 2 atm, whose effective area measured μA = 18.97 mm^2; the air flowrate was $G_{air\ jet} = 8.7 \cdot 10^{-3}$ kg/s, the ejected gas flowrate was $G_{air\ eject} = 42 \cdot 10^{-3}$ kg/s, the flowrate of the isotactic polypropylene melt was G_{pp} = 16.2 kg/h. The value of the similarity criteria, characterizing the process of pneumatic spraying of the polypropylene melt in the presence of nanoparticle aerosol, are: the Weber criterion for a jet; characterizes the ratio of inertia-to-surface tension forces $We_j = 6.4 \cdot 10^3$; the Reynolds criterion for a jet; characterizes the ratio of inertia-to-friction (viscosity) forces $Re_j = 27.2 \cdot 10^3$ and the Laplace criterion for a jet; characterizes the ratio of surface tension-to-friction (viscosity) forces $Lp_j = 6.4 \cdot 10^{-8}$. A high value of the Weber criterion suggests that disintegration of the molten jet occurs via the mechanism of separation. From the value of the Laplace criterion one can make a conclusion that predominating influence on the spraying process belongs to the polymer melt viscosity with respect to the surface tension forces. The Reynolds

criterion characterizes the air flow in the regime of floatation around the melt jet, whose considerable turbulence favours homogeneous distribution of nanoparticles over the polymer melt surface.

High viscosity of the melt inhibits particle diffusion from the polymer surface into the bulk; hence the polymer particles as a result of structural-phase transformations get attached to the surface. A rigid attachment of the ATO nanoparticles on the fiber material has been verified by the data of atomic-emission spectrometry in an ICAP 6300 Duo Thermo Spectrometer using inductively coupled plasma. This method allowed demonstrating that the content of tin in the nanoparticles on the polypropylene fiber does not change after its flushing with flowing water.

4. Summary and conclusion

In accordance with our findings it is established that synthesis conditions of the ATO, ITO, and BTO particles optimal from a perspective of the environmental safety and thermodynamic stability of materials as well as of achievement of a predetermined concentration of free charge carriers in them are found. These conditions are provided by using the "reverse" hydrolytic co-precipitation of hydroxides from chloride solutions combined with the subsequent thermal treatment at 1000°C.

Thus, the method of spraying a freely outflowing stream of a molten thermoplastic polymer by gas in presence of nanoparticles makes it possible to produce fibres containing disperse oxides of rare and trace elements on theirs surfaces. Oxide nanoparticles, a significant part of each of them extends beyond the polymer, with the sizes less than 100 nm and a predetermined concentration of free charge carriers can be used to impart to the fibre materials the pre-designed catalytic, photosensitive as well as heat and sound insulating properties.

Acknowledgments

This study has been performed under the financial support of the Ministry of Science and Education of the Russian Federation within the framework of the government contract No. 16.3037.2017/4.6.

References

[1] Miyake S 2005 Novel Materials Processing by Advanced Electromagnetic Energy Sources *MAPEES 04* (Elsevier Ltd, London) 345

[2] Yoo B, Kim K, Lee S H, Kim W M and Park N G 2008 ITO/ATO/TiO_2 triple-layered transparent conducting substrates for dye-sensitized solar cells *Sol Energy Mater and Sol Cells* **92(8)** 873-877

[3] Jeong H, Oh H M, Bang S, Jeong H J, An S J, Han G H, Jeong M S et al 2016 Metal-Insulator-Semiconductor Diode Consisting of Two-Dimensional Nanomaterials *Nano. Lett.* **16** 1858

[4] Zhang J and Gao L 2004 Synthesis and characterization of antimony-doped tin oxide (ATO) nanoparticles by a new hydrothermal method *Mater. Chem. and Phys.* **87** 10-13

[5] Yang H, Qiu G, Zhang X, Tang A and Yang W 2004 Preparation of CdO nanoparticles by mechanochemical reaction *J. of Nanopart. Res.* **6** 539-542

[6] Xiong Y, Zhang G, Zhang S, Zeng D and Xie C 2014 Tin oxide thick film by doping rare earth for detecting traces of CO_2: Operating in oxygen-free atmosphere *Mater. Res. Bull.* **52** 56-64

[7] Mohapatra H S, Chatterjee A and Kumar P 2013 New Generation Application of Polypropylene Fibre *Int. J. of Adv. and Nano Technol.* **1** 2347-6389

[8] Shi L, Kang W M, Zhuang X P and Cheng B W 2011 Preparation and Properties of PP Melt-Blown Nonwoven Wadding Blended PET Crimp Fibers *Adv. Mater. Res.* **334** 1287-1290

[9] Pinchuk L S, Goldade V A, Makarevich A V and Kestelman V N 2002 *Melt Blowing: Equipment, Technology, and Polymer Fibrous Materials* (Springer, Berlin) 212

[10] Lysak I A, Lysak G V, Malinovskaya T D, Tchaikovskaya O N and Artyushin V R 2015 Photodegradation of an Herbicide (2-methyl-4-chlorophenoxyacetic acid) in the Presence of "TiO_2, SnO_2, SnO_2/TiO_2 Nanoparticles – Polypropylene Fibrous Carrier" Systems *Adv. Mater. Res.* **1085** 107-112

[11] Lysak I A, Malinovskaya T D, Lysak G V, Potekaev A I, Kulagina V V and Tazin D I 2017 Formation of Fiber Materials by Pneumatic Spraying of Polymers in Viscous-Flow States *Rus. Phys. J.* **59(10)** 1581–1588
[12] Lysak I A, Malinovskaya T D, Lysak G V, R.F. Patent No. 2,624,189 (1 March 2016)
[13] Zakharova A A, Vekhter E V, Shklyar A V and Pak A J 2018 Visual modeling in an analysis of multidimensional data *J. of Phys.: Conf. Series* **944(1)** 5.
[14] Zakharova A A, Vekhter E V and Shklyar A V 2017 Methods of solving problems of data analysis using analytical visual models *Scientific Visualization* **9(4)** 78-88
[15] Zakharova A A, Vekhter E V, Shklyar A V and Zavyalov D 2017 Visual detection of internal patterns in the empirical data *Communications in Computer and Information Science* **754** 215-230
[16] Lysak G V, Lysak I A, Malinovskaya T D and Volokitin G G 2010 Microwave synthesis of SnO_2 nanocrystals on the surface of fine polymer fibers *Inorg Mater* **46(2)** 183-186